Ferroelectrics

ISSN: 0015-0193 (Print) 1563-5112 (Online) Journal homepage: https://www.tandfonline.com/loi/gfer20

Physical properties of strontium barium niobate thin films prepared by polymeric chemical method

M. Melo, E.B. Araujo, A.P. Turygin, V.Ya. Shur & A.L. Kholkin

To cite this article: M. Melo, E.B. Araujo, A.P. Turygin, V.Ya. Shur & A.L. Kholkin (2016) Physical properties of strontium barium niobate thin films prepared by polymeric chemical method, Ferroelectrics, 496:1, 177-186, DOI: 10.1080/00150193.2016.1155035

To link to this article: https://doi.org/10.1080/00150193.2016.1155035

FERROELECTRICS
2016, VOL. 496, 177–186
http://dx.doi.org/10.1080/00150193.2016.1155035

Taylor & Francis
Taylor & Francis Group

Physical properties of strontium barium niobate thin films prepared by polymeric chemical method

M. Melo[a], E.B. Araujo[a], A.P. Turygin[b], V.Ya. Shur[b], and A.L. Kholkin[b,c]

[a]Department of Physics and Chemistry, São Paulo State University, Ilha Solteira, SP, Brazil; [b]Institute of Natural Sciences, Ural Federal University, Ekaterinburg, Russia; [c]Department of Physics & CICECO – Aveiro Institute of Materials, University of Aveiro, Aveiro, Portugal

ABSTRACT

Randomly oriented $Sr_{0.75}Ba_{0.25}Nb_2O_6$ thin films have been deposited on Pt(111)/Ti/SiO_2/Si substrates using a polymeric chemical method to study their physical properties. Refinements of the structure confirm the stoichiometry of the studied films. The relaxor behavior is evidenced by the dielectric measurements and Vögel-Fulcher analysis of the dielectric curves. Lowering the transition temperature (T_m) by about 100 K and asymmetries in the local hysteresis loops well above T_m are discussed in terms of the existence of complex defects in thin films.

ARTICLE HISTORY
Received 29 August 2015
Accepted 30 October 2015

KEYWORDS
Relaxor; hysteresis loop; dielectric measurement; SBN

1. Introduction

Strontium barium niobate $Sr_xBa_{1-x}Nb_2O_6$ (SBN) is an important ferroelectric material from the scientific and technological points of view. SBN is a solid solution in the binary $SrNb_2O_6$-$BaNb_2O_6$ system, has a tetragonal tungsten-bronze structure described by the general formula AB_2O_6 and exhibits the spontaneous polarization oriented along the *c*-direction. Due to its excellent pyroelectric coefficient [1], piezoelectric [2] and electro-optic [3, 4] properties, SBN is a promising material for a number of technological applications.

The structure of SBN has been studied in detail by Jamieson *et al.* [5] in the late 1960s. It consists of NbO_6 octahedra sharing corners so that the interstitial sites A1 and A2 result. Nb^{5+} atoms occupy B1 and B2 sites in this structure, Sr^{2+} atom in the A1 site has 12 nearest oxygen atoms in distorted cube-octahedral coordination, while Ba^{2+}/Sr^{2+} atoms in the A2 site are surrounded by nine nearest-neighbor oxygen atoms and this arrangement may be described as distorted tricapped trigonal prismatic coordination [5]. Since there are six positions to be occupied in the A sites, one position remains unoccupied introducing a charge disorder in the structure [6]. As this disorder is associated with Sr^{2+} attributed to atom in the structure, it is expected an increase in the charge disorder leading to a relaxor behavior in SBN with higher strontium content in the composition.

The growing demand for portability in consumer electronics and integrated optical devices has stimulated the use of SBN in the thin film form as well as studies to understand the

CONTACT E.B. Araujo eudes@dfq.feis.unesp.br

Color versions of one or more of the figures in the article can be found online at www.tandfonline.com/gfer.

influence of size effects, defects, and other extrinsic factors on their physical properties. Often, the physical properties of the ferroelectric thin films were found to be more influenced by the small grain size rather than the interface effects [7]. Nevertheless, some papers have focused on the influence of strain imposed by the substrate and films thickness on their performance [8, 9]. However, the true origin (either microscopic or mesoscopic) of the intriguing dielectric properties of ferroelectric thin films still remains not understood and needs additional investigations [10]. In this context, the used polymeric method for thin films deposition plays an important role to control defects and tailor their properties.

SBN thin films have been deposited by various techniques such as sol-gel [11, 12], rf-sputtering [13, 14], pulsed laser deposition [15, 16], and metal-organic chemical vapor deposition [17, 18]. The results vary strongly from one method to another, especially concerning dielectric and ferroelectric properties. Although the search for new routes for thin film preparation remains an interesting and open subject to obtain films of high quality, understanding the specificity of each technique is an important point to control and optimize the physical properties of thin films. Recently, we have observed the existence of an imprint effect [19], responsible for limiting the lifetime and failure of ferroelectric memory devices, in $Pb(Zr_{0.50}Ti_{0.50})O_3$ (PZT) thin films deposited by an alternative polymeric chemical method [20]. Considering the imprint as one of intrinsic effects of this deposition method, the study of the physical properties of SBN thin films deposited by the same polymeric route has motivated the present work.

2. Experimental

In the present work, SBN thin film with nominal $Sr_{0.75}Ba_{0.25}Nb_2O_6$ composition has been prepared using a polymeric chemical route based on the Pechini method [21]. Barium carbonate $BaCO_3$ (Aldrich), strontium carbonate $SrCO_3$ (Aldrich), and niobium ammonium oxalate $NH_4H_2NbO(C_2O_4).3H_2O$ (CBMM, Brazil) were used as starting reagents. Initially, niobium ammonium oxalate was dissolved at 40°C for 10 minutes in aqueous solution of citric acid (CA) to form niobium citrate. After homogenization of this solution, ethylene glycol (EG) was added to promote polymerization of mixed citrate by polyestherification reaction at 90°C for 30 minutes. Cooling this solution at room temperature, a transparent resin is obtained. Next, dissolving together the strontium and barium carbonates at the same conditions in a separate solution of citric acid, a citrate solution is formed. Adding ethylene glycol to this citrate solution, the polyestherification reaction occurs at the same temperature to obtain another transparent resin. In both cases, the CA/Metal molar ratio was fixed at 5/1, while the CA/EG ratio was fixed as 40/60 (in mol%). Subsequently, both resins are mixed at room temperature and stirred for 1 hour for homogenization. After adjusting viscosity with distilled water, a clear polymeric resin is finally obtained. The final transparent resin indicates that all metallic ions were distributed throughout the polymeric resin.

Films of polymeric resins are initially deposited by spin coating on $Pt/Ti/SiO_2/Si(100)$ substrates at 6000 rpm for 20 s. The pyrolysis is performed in air putting the deposited films directly on a hot plate at ~200°C for 10 minutes and then in a conventional electric furnace at 400°C for 30 minutes. The film thickness increases with the deposition of more layers on the previous pyrolyzed film. The same heat annealing procedure was repeated to remove the organics. After obtaining the required film thickness, a final heat annealing at 700°C for

1 hour promotes the film crystallization. The obtained film is uniform and crack-free with 550 nm in thickness.

X-ray diffraction (XRD) patterns of the SBN films have been obtained at room temperature using a Rigaku Ultima IV diffractometer with CuK_α (1.5406 Å) radiation. Rietveld [22] refinements were performed with the XRD data to obtain information about the SBN structure. Initially, XRD data were input into the GSAS [23] structure refinement code under the EXPGUI interface [24]. Peak profiles were fitted using the Thompson-Cox-Hastings [25] pseudo-Voigt function, while a sixth-order polynomial was used to fit the background. We consider a pure tetragonal phase with P4bm space group and the initial parameters refined for SBN single crystal by Jamieson *et al.* [5]. The main criteria for judging the quality of the fitting is the final fit of the calculated pattern compared to the observed data. The R-factors weighted profile R_{wp}; the statistically expected R_{exp} and the goodness-of-fit (GOF) indices $\chi^2 = R_{wp} / R_{exp}$ are usually used to attest the fit quality [26].

Dielectric permittivity measurements were performed in vacuum using an Agilent 4284A LCR meter in the frequency 10–600 kHz and temperature 50–400 K ranges. For these measurements, several gold electrodes (0.3 mm in diameter) were deposited through a mask over a 1×1 cm^2 area of the films in order to form capacitors. The topography, piezoresponse, and local hysteresis loops measurements were performed with a scanning probe microscope MFP-3D (Asylum Research, Oxford Instruments, USA) using the probes ASYLEC-01 with titanium-iridium conductive coating (Asylum Research, Oxford Instruments, USA) with a radius of curvature 28 nm, resonance frequency 70 kHz, and spring constant 2 N/m. Piezoresponse measurements were performed in a PFM mode with 3V AC near resonance frequency (296 kHz). Local hysteresis loops were measured with 5, 10, and 15 maximum DC voltages (2 s per loop cycle).

3. Results and discussion

Fig. 1 shows the observed, calculated, and difference profiles obtained by Rietveld refinements of the XRD data for polycrystalline randomly oriented SBN thin films. The indexed

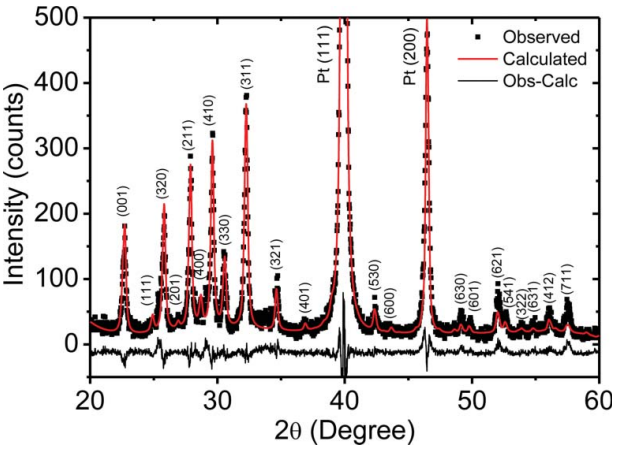

Figure 1. Observed (dots), calculated (red lines), and difference (bottom lines) XRD profiles of $Sr_{0.75}Ba_{0.25}Nb_2O_6$ thin film.

(*hkl*) peaks refer to the tetragonal phase of the SBN with *P*4*bm* space group. The peaks of Pt (111) and Pt(200) refer to the cubic phase of the platinum substrate with space group $Fm\bar{3}m$ and lattice parameter $a = 3.892$ Å. Table 1 summarizes the position, atom coordinates, and lattice parameters of the SBN structure obtained from refinements. The crystallographic R-factors and goodness of fit (χ^2) are also included in Table 1. Good agreement between the observed and calculated patterns in Fig. 1 and the obtained small value $\chi^2 = 1.7$ indicate a good fit. Consequently, it is concluded that structural parameters and calculated lattice parameters summarized in Table 1 are representative values for the SBN films studied in the present work. The refined lattice parameters $a = 12.4243$ Å and $c = 3.9082$ Å are similar to those obtained for SBN single crystals with the same nominal composition (Sr = 0.75) [5].

Fig. 2a shows the temperature dependences of the real (ε') and imaginary (ε'') parts of the dielectric permittivity in the frequency range 10–600 kHz. The maximum value observed for the ε' decreases with increasing frequencies and the temperature maximum, T_m, shifts to higher temperatures displaying the frequency and temperature dispersions, characteristic of a relaxor material. For the frequencies 10 and 600 kHz, the T_m values were 221 and 236 K, respectively, demonstrating a difference of about 15 K. In addition, the ε' temperature maximum (T_m) also shifts to higher values with frequency and temperature increase, as observed in Fig. 2a.

The maximum temperature $T_m = 221$ K (at 10 kHz) observed in Fig. 2a is lower by 100 K as compared to that reported for SBN single crystals ($T_m = 320$ K, at 10 kHz) with the same composition of Sr = 0.75 [27]. A similar result has been reported in SBN films deposited by pulsed laser deposition, where the phase transition occurring well below that in single crystals was attributed to larger defect concentrations in the film [28]. The transition to a ferroelectric state in relaxors is very sensitive to any disorder inducing factor and, as a consequence, the shift in phase transition temperature to lower temperatures is a phenomenon observed not only in SBN, but in other relaxors as well [29]. Often, the origin of the phase transition lowering has been attributed to different external factors, such as doping, stoichiometry, grain size distribution, tensile/compressive strain, and existence of a non-active thin layer in the film/substrate interface. The decrease of the transition temperature in SBN system (ceramics or single crystals) with increasing Sr content was attributed to the increase in disorder [30]. Thus, it is reasonable to consider defects associated with disorder in the SBN system as a natural mechanism responsible for lowering phase transition temperatures. The presence of point defects, such as complex vacancies in other ferroelectric thin

Table 1. Summary of Rietveld refinement results for $Sr_{0.75}Ba_{0.25}Nb_2O_6$ film at room temperature. Parameters refined for tetragonal phase with P4bm space group.

Atom	x	y	z	Position	Occupancy
Nb(1)	0.0000	0.5000	0.0236	2b	1.00
Nb(2)	0.0747	0.21148	0.0089	8d	1.00
Sr(1)	0.0000	0.0000	0.5000	2a	0.82
Sr(2)	0.17236	0.6724	0.5069	4c	0.50
Ba(1)	0.17236	0.6724	0.5069	4c	0.34
O(1)	0.3450	0.0049	−0.0546	8d	1.00
O(2)	0.1369	0.0679	0.0663	8d	1.00
O(3)	0.2800	0.7800	−0.0356	4c	1.00
O(4)	−0.0155	0.4845	0.5093	4c	0.50
O(5a)	0.3092	0.4024	0.4795	8d	0.50
O(5b)	0.2792	0.4364	0.5023	8c	0.50
Lattice parameters: $a = 12.4243$ Å; $c = 3.9082$ Å					
GOF and R-factors: $\chi^2 = 1.7$ $R_{wp} = 14.0$ $R_p = 9.1$					

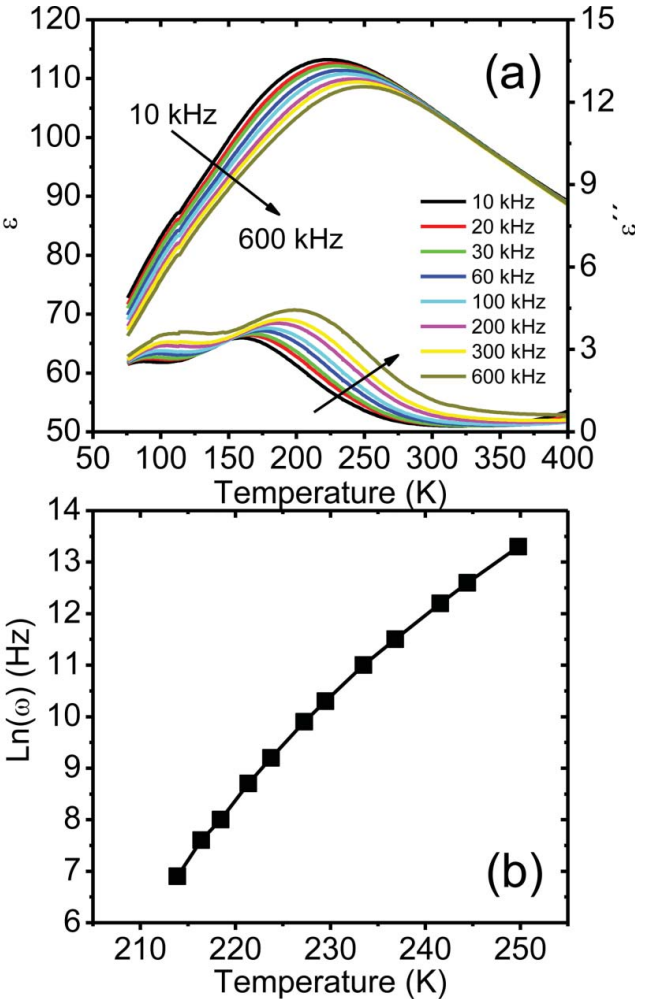

Figure 2. (a) Real and imaginary dielectric permittivities of SBN thin film as a function of temperature at measurement frequencies of 10, 20, 30, 60, 100, 200, 300, and 600 kHz. (b) Inverse of the temperature of the dielectric maximum as a function of the measurement frequency.

films [20] deposited by the polymeric chemical method, suggest a probable origin for the disorder increasing in our SBN films and the observed shift in the phase transition.

In many relaxor ferroelectrics, the relationship between the probe frequency ω and the temperature of dielectric maximum T_m can be described by the Vögel-Fulcher (VF) equation [31, 32]:

$$\omega = \omega_0 \exp\left[-\frac{E_a}{k_B(T_m - T_f)}\right], \tag{1}$$

where ω_0 is the attempt frequency, T_f is the static freezing temperature, k is the Boltzmann constant, and E_a is the activation energy.

We fit the experimental data by Eq. (1) as it is shown in Fig. 2b. A good agreement between experimental data (points) and fitting (solid line) in Fig. 2b suggests that relaxor behavior in SBN film is analogous to a spin glass with polarization fluctuations above static

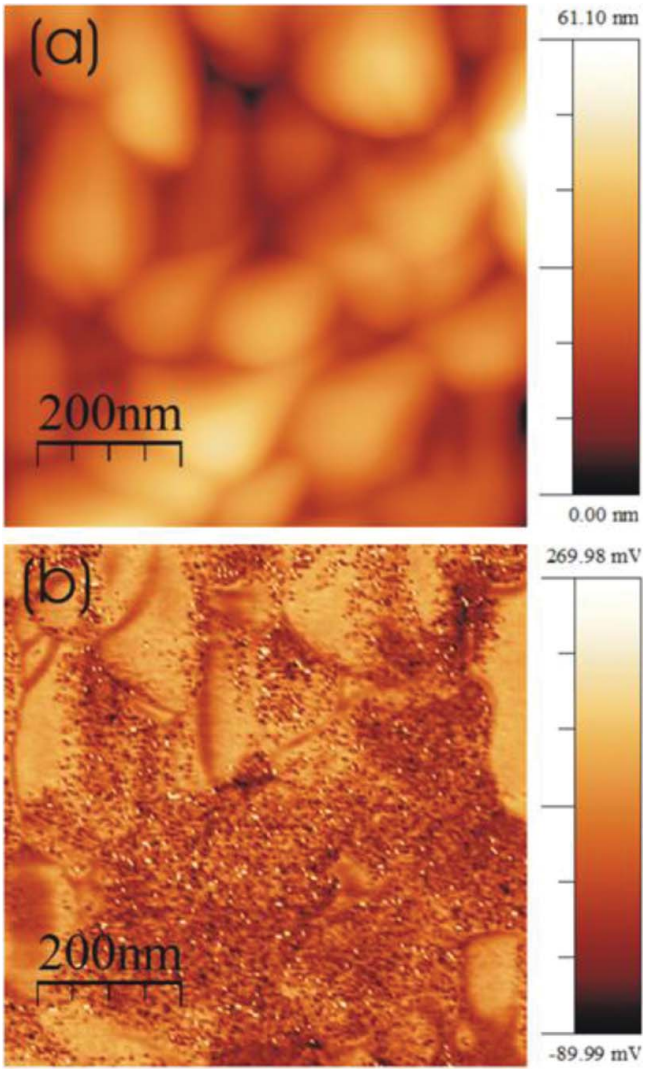

Figure 3. (a) Topography and (b) piezoresponse image of SBN thin film.

freezing temperature and similar to that observed in classic lead magnesium niobate (PMN) relaxor ferroelectric [31]. The obtained fitting parameters for SBN films were $\omega_0 = 1.0\times10^{10}$Hz, $T_f = 179$ K, and $E_a = 0.0038$ eV. Comparing these results with those reported in the literature for single crystals of the same composition, $\omega_0 = 1.6\times10^{9}$ Hz, $T_f = 304$ K and $E_a = 0.015$ eV, we found that our results for thin films are slightly different. While E_a and T_f are smaller than in single crystals, the attempt frequency ω_0 is almost an order of magnitude greater. Apparent change in these parameters is a natural consequence of lowering phase transition in the SBN films.

The topography of the studied SBN thin film is shown in Fig. 3a, while Fig. 3b displays the corresponding piezoresponse image of the film. The topography is characterized by elongated grains with average grain size around 200 nm and root mean square (RMS) roughness 31 nm. Although not shown, the topography measure in different places of the studied film

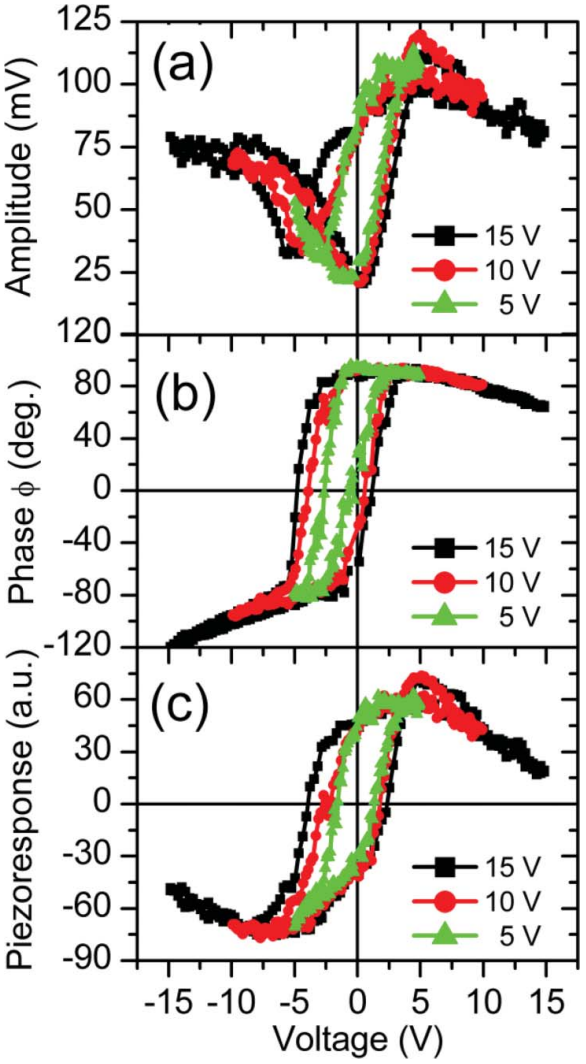

Figure 4. (a) Amplitude, (b) phase, and (c) piezoresponse curves of SBN thin film at different voltages.

is nearly the same. Three types of contrasts, bright, dark, and "noisy", are observed in the piezoresponse image in Fig. 3b. The noisy contrast in the piezoresponse could be attributed to very fine polar structures in the SBN film, probably associated with polar nanoregions (PNRs). However, considering that under PFM experimental conditions the dimensions less than 10 nm cannot be resolved; it is very difficult to prove that these noisy areas can be indeed assigned to PNRs in the studied film.

Fig. 4 shows the amplitude, phase, and the piezoresponse curves of the studied SBN film recorded at room temperature. Typical butterfly and local hysteresis loops are shown in this figure for three different DC voltages. The observation of local hysteresis loops well above the maximum temperature ($T_m = 221$ K) in Fig. 4c is a clear signature of non-zero polarization in the studied SBN film. Contrary to normal ferroelectrics, for which polarization becomes zero at the Curie temperature, the hysteresis loops are observed above the transition

temperature, which is often attributed to the presence of polar regions in relaxors [33]. It is expected that the formation of these polar regions occurs at Burns temperature (T_B), which can be hundreds of degrees above T_m [34]. Consequently, ferroelectric hysteresis loops are also observed well above T_m in relaxor thin films with perovskite structure [35], as well as in relaxor ceramics in the Aurivillius family [36]. Initial models proposed the quantification of the hysteretic behavior in relaxor ferroelectrics above the freezing temperature [37], while more recent models incorporate temperature effects inherent to relaxor ferroelectric [38].

Apart of the existence of hysteresis loops above the transition temperature (Fig. 4c), the asymmetry observed in these local hysteresis loops is another point to be considered. In Fig. 4c, the coercive voltage shifts to negative values ($\Delta V_c = -1.54$ V), while the piezoresponse amplitude shifts to positive values. These asymmetries are a signature of the imprint effect, defined as the tendency of one polarization state to become more stable than the opposite one [39]. The imprint mechanisms for different ferroelectric systems have been often discussed in terms of alignment of defect dipoles (oxygen vacancies, holes, cation vacancies) and within interface screening models [40, 41]. Recent studies have demonstrated a clear imprint effect in PZT thin films prepared by the polymeric chemical method [42]. This effect has been characterized by an effective electric field in these films, probably due to defects (complex oxygen vacancies). Thus, it is reasonable to assume that similar effect will present in SBN thin films deposited by the polymeric method, as in fact demonstrated in Fig. 4c. Then, despite of any conclusive result on the origin of the imprint effect in the SBN films, the asymmetry observed in the local hysteresis loops suggests the presence of an internal electric field. The decrease of piezoresponse observed at high voltages in Fig. 4c is not yet clear. Probably, it is an electrochemistry effect associated with local reduction/oxydation or with interaction of complex defects with applied electric field. Therefore, further experiments are needed to corroborate or refute the origin of this behavior.

4. Conclusion

In summary, $Sr_{0.75}Ba_{0.25}Nb_2O_6$ thin films have been deposited using a polymeric chemical method in order to study their physical properties. Rietveld refinements of the structure confirm the stoichiometry and the tetragonal structure of the studied film. Vögel-Fulcher analysis revealed clear relaxor behavior of the material. As opposed to single crystals of the same composition, apparent lowering of the transition temperature (T_m = 221 K), i.e. by about 100 K, has been observed. Local hysteresis loops persist well above the T_m, which is a clear indication of the existence of non-zero polarization in the SBN film at room temperature. Finally, asymmetries of the local hysteresis loops suggest an imprint effect in the studied film.

Acknowledgments

The equipment of the Ural Center for Shared Use “Modern nanotechnology” UrFU was used.

Funding

We would like to express our gratitude to the Brazilian agencies FAPESP (Projects 2010/16504-0 and 2007/08534-3) and CNPq (Research grant 305973/2012–6 and Project 400677/2014–8) for their

financial support. This work was also developed in the scope of the project CICECO – Aveiro Institute of Materials (Ref. FCT UID/CTM/50011/2013), financed by national funds through the FCT/MEC and when applicable co-financed by FEDER under the PT2020 Partnership Agreement. The research was made possible in part by the Ministry of Education and Science of the Russian Federation (UID RFMEFI59414X0011) by Government of the Russian Federation (Act 211, Agreement 02. A03.21.0006).

References

1. A. M. Glass, Investigation of the electrical properties of $Sr_{1-x}Ba_xNb_2O_6$ with special reference to pyroelectric detection. *J Appl Phys.* **40**, 4699–4713 (1969).
2. J. D. Zook, and S. T. Liu, Pyroelectric effects in thin film. *J Appl Phys.* **49**, 460–4606 (1978).
3. S. Sakamoto, and T. Yazaki, Anomalous electro−optic properties of ferroelectric strontium barium niobate and their device applications. *Appl Phys Lett.* **22**, 429–431 (1973).
4. M. Horowitz, A. Bekker, and B. Fischer, Broadband second−harmonic generation in $Sr_xBa_{1-x}Nb_2O_6$ by spread spectrum phase matching with controllable domain gratings. *Appl Phys Lett.* **62**, 2619–2621 (1993).
5. P. B. Jamieson, S. C. Abrahams, and J. L. Bernstein, Ferroelectric tungsten bronze-type crystal structures. *I. Barium strontium niobate $Ba_{0.27}Sr_{0.75}Nb_2O_{5.78}$. J Chem Phys.* **48**, 5048–5057 (1968).
6. M. S. Kim, P. Wang, J. H. Lee, J. J. Kim, H. Y. Lee, and S. H. Cho, Site occupancy and dielectric characteristics of strontium barium niobate ceramics: Sr/Ba ratio dependence. *Jpn J Appl Phys.* **41**, 7042–7047 (2002).
7. M. Tyunina, J. Levoska, S. Leppavuori, and A. Stemberg, Dielectric properties of pulsed laser deposited films of $PbMg_{1/3}Nb_{2/3}$-$PbTiO_3$ and $PbSc_{1/2}Nb_{1/2}O_3$-$PbTiO_3$ relaxor ferroelectrics. *J Appl Phys.* **86**, 5179–5184 (1999).
8. N. A. Pertsev, A. G. Zembilgotov, and A. K. Tagantsev, Effect of mechanical boundary conditions on phase diagrams of epitaxial ferroelectric thin films. *Phys Rev Lett.* **80**, 1988–1981 (1998).
9. N. A. Pertsev, A. K. Tagantsev, and N. Setter, Phase transitions and strain-induced ferroelectricity in $SrTiO_3$ epitaxial thin films. *Phys Rev B.* **61**, R825–R829 (2000).
10. T. M. Shaw, S. Trolier-McKinstry, and P. C. McIntyre, The properties of ferroelectric films at small dimensions. *Annu Rev Mater Sci.* **30**, 263–298 (2000).
11. Y. Xu, C. J. Chen, R. Xu, and J. D. Mackenzie, Ferroelectric $Sr_{0.60}Ba_{0.40}Nb_2O_6$ thin-films by the sol-gel process - electrical and optical-properties. *Phys Rev B.* **44**, 35–41 (1991).
12. S. Hirano, T. Yogo, K. Kikuta, and K. Ogiso, Preparation of strontium barium niobate by sol-gel method. *J Am Ceram Soc.* **75**, 1697–1700 (1992).
13. M. Cuniot-Ponsard, J. M. Desvignes, B. Ea-Kim, and E. Leroy, Radio frequency magnetron sputtering deposition of hetero-epitaxial strontium barium niobate thin films ($Sr_xBa_{1-x}Nb_2O_6$). *J Appl Phys.* **93**, 1718–1724 (2003).
14. Y. Yin, X. H. Fu, and H. Ye, Growth and properties of highly orientated $Sr_{0.75}Ba_{0.25}Nb_2O_6$ thin films on silicon substrates with MgO or TiN buffer layers. *Thin Solid Films*. **519**, 6403–6407 (2011).
15. S. S. Thöny, K. E. Youden, J. S. Harris, and L. Hesselink, Growth of epitaxial strontium barium niobate thin films by pulsed laser deposition. *Appl Phys Lett.* **65**, 2018–2020 (1994).
16. X. L. Guo, Z. G. Liu, X. Y. Chen, S. N. Zhu, S. B. Xiong, W. S. Hu, and C. Y. Lin, Pulsed laser deposition of $Sr_xBa_{1-x}Nb_2O_6$/MgO bilayered films on Si wafer in waveguide farm. *J Phys D Appl Phys.* **29**, 1632–1635 (1996).
17. M. J. Nystrom, B. W. Wessels, W. P. Lin, G. K. Wong, D. A. Neumayer, and T. J. Marks, Nonlinear optical properties of textured strontium barium niobate thin films prepared by metalorganic chemical vapor deposition. *Appl Phys Lett.* **66**, 1726–1728 (1995).
18. M. K. Lee, and R. S. Feigelson, Growth of epitaxial strontium barium niobate thin films by solid source metal-organic chemical vapor deposition. *J Crystal Growth.* **180**, 220–228 (1997).
19. W. L. Warren, B. A. Tuttle, D. Dimos, G. E. Pike, H. S. Al-Shareef, R. Ramesh, and J. T. Evans, Imprint in ferroelectric capacitors. *Jpn J Appl Phys.* **35**, 1521–1524 (1996).

20. E. C. Lima, E. B. Araujo, A. G. Souza, A. R. Paschoal, I. K. Bdikin, and A. L. Kholkin, Structural depth profile and nanoscale piezoelectric properties of randomly oriented $Pb(Zr_{0.50}Ti_{0.50})O_3$ thin films. *J Phys D Appl Phys.* **45**, 215304 (2012).
21. M. Pechini, U. S. Pat. No 3 330 697, (July 11 1967).
22. H. M. Rietveld, Line profiles of neutron powder-diffraction peaks for structure refinement. *Acta Crystallogr.* **22**, 151–152 (1967).
23. A. C. Larson, and R. B. Von Dreele, General structure analysis system (GSAS). *Los Alamos National Laboratory Report LAUR.* 86–748 (1994).
24. B. H. Toby, EXPGUI, a graphical user interface for GSAS. *J Appl Cryst.* **34**, 210–213 (2001).
25. P. Thompson, D. E. Cox, J. B. Hastings, Rietveld refinement of Debye-Scherrer synchrotron X-ray data from Al_2O_3. *J Appl Crystallogr.* **20**, 79–83 (1987).
26. L. B. McCusker, R. B. Von Dreele, D. E. Cox, D. Louer, and P. Scardi, Rietveld refinement guidelines. *J Appl Cryst.* **32**, 36–50 (1999).
27. I. Bhaumik, S. Ganesamoorthy, R. Bhatt, N. Subramanian, A. K. Karnal, P. K. Gupta, S. Takekawa, and K. Kitamura, Influence of cerium doping on the dielectric relaxation of $Sr_{0.75}Ba_{0.25}Nb_2O_6$ single crystal grown by the double crucible Stepanov technique. *J Alloys Compd.* **621**, 26–29 (2015).
28. A. Infortuna, P. Muralt, M. Cantoni, A. Tagantsev, and N. Setter, Microstructural and electrical properties of $(Sr,Ba)Nb_2O_6$ thin films grown by pulsed laser deposition. *J Eur Ceram Soc.* **24**, 1573–1577 (2004).
29. F. Chu, N. Setter, and A. K. Tagantsev, The spontaneous relaxor−ferroelectric transition of $Pb(Sc_{0.5}Ta_{0.5})O_3$. *J Appl Phys.* **74**, 5129–5134 (1993).
30. S. Ganesamoorthy, I. Bhaumik, R. Bhatt, A. K. Karnal, P. K. Gupta, S. Kumaragurubaran, R. Mohankumar, K. Kitamura, S. Takekawa, and M. Nakamura, A comparative study of dielectric relaxation in $Sr_{0.61}Ba_{0.39}Nb_2O_6$ and $Sr_{0.75}Ba_{0.25}Nb_2O_6$ single crystals. *Jpn J Appl Phys.* **47**, 1012–1015 (2008).
31. D. Viehland, S. J. Jang, L. E. Cross, and M. Wuttig, Freezing of the polarization fluctuations in lead magnesium niobate relaxors. *J Appl Phys.* **68**, 2916–2921 (1990).
32. A. K. Tagantsev, Vogel-Fulcher relationship for the dielectric permittivity of relaxor ferroelectrics. *Phys Rev Lett.* **72**, 1100–1103 (1994).
33. L. E. Cross, Relaxor ferroelectrics. *Ferroelectrics.* **76**, 241–267 (1987).
34. G. Burns, and F. H. Dacol, Crystalline ferroelectrics with glassy polarization behavior. *Phys Rev B.* **28**, 2527–2530 (1983).
35. A. Dixit, S. B. Majumder, R. S. Katiyar, and A. S. Bhalla, Relaxor behavior in sol-gel-derived $BaZr_{(0.40)}Ti_{(0.60)}O_3$ thin films. *Appl Phys Lett.* **82**, 2679–2681 (2003).
36. S. Kumar, D. A. Ochoa, J. E. Garcia, and K. B. R. Varma, Relaxor Ferroelectric Behavior and Structural Aspects of $SrNaBi_2Nb_3O_{12}$ ceramics. *J Am Ceram Soc.* **95**, 1339–1342 (2012).
37. A. E. Glazounov, A. J. Bell, A. K. Tagantsev, Relaxors as superparaelectrics with distributions of the local transition-temperature. *J Phys Condens Matter.* **7**,4145–4168 (1995).
38. J. K. Raye, and R. C. Smith, A temperature-dependent hysteresis model for relaxor ferroelectric compounds. *Proc. SPIE 5383, Smart Structures and Materials 2004: Modeling, Signal Processing, and Control*, **1** (July 26, 2004).
39. H. N. Al-Shareef, D. Dimos, W. L. Warren, and B. A. Tuttle, Voltage offsets and imprint mechanism in $SrBi_2Ta_2O_9$ thin films. *J Appl Phys.* **80**, 4573–4577 (1996).
40. M. Grossmann, O. Lohse, D. Bolten, U. Boettger, T. Schneller, and R. Waser, The interface screening model as origin of imprint in $PbZr_xTi_{1-x}O_3$ thin films. *I. Dopant, illumination, and bias dependence. J Appl Phys.* **92**, 2680–2687 (2002).
41. A. Gruverman, B. J. Rodriguez, R. J. Nemanich, and A. I. Kingon, Nanoscale observation of photoinduced domain pinning and investigation of imprint behavior in ferroelectric thin films. *J Appl Phys.* **92**, 2734–2739 (2002).
42. E. B. Araujo, E. C. Lima, I. K. Bdikin, and A. L. Kholkin, Thickness dependence of structure and piezoelectric properties at nanoscale of polycrystalline lead zirconate titanate thin films. *J Appl Phys.* **113**, 187206 (2013).